Measurement of the optical absorption spectra of epitaxial graphene from terahertz to visible

Jahan M. Dawlaty,[1,a] Shriram Shivaraman,[1] Jared Strait,[1] Paul George,[1] Mvs Chandrashekhar,[1] Farhan Rana,[1] Michael G. Spencer,[1] Dmitry Veksler,[2] and Yunqing Chen[2]
[1]*School of Electrical and Computer Engineering, Cornell University, Ithaca, New York 14853, USA*
[2]*Center for Terahertz Research, Rensselaer Polytechnic Institute, Troy, New York 12180, USA*

(Received 13 August 2008; accepted 8 September 2008; published online 30 September 2008)

We present experimental results on the optical absorption spectra of epitaxial graphene from the visible to the terahertz frequency range. In the terahertz range, the absorption is dominated by intraband processes with a frequency dependence similar to the Drude model. In the near-IR range, the absorption is due to interband processes and the measured optical conductivity is close to the theoretical value of $e^2/4\hbar$. We extract values for the carrier densities, the number of carbon atom layers, and the intraband scattering times from the measurements. © *2008 American Institute of Physics*. [DOI: 10.1063/1.2990753]

Graphene is a single atomic layer of carbon atoms forming a honeycomb crystal lattice.[1,2] The unusual electronic and optical properties of graphene have generated interest in both experimental and theoretical arenas.[2–6] The high mobility of electrons in graphene has prompted a large number of investigations into graphene based high speed electronic devices such as field-effect transistors and *p-n* junction diodes, photonic devices, such as terahertz oscillators, and low noise sensors.[4,7–11] For many of these applications, knowledge of the optical properties of graphene is critical.

Recently, epitaxial growth of graphene by thermal decomposition of SiC surface at high temperatures has been demonstrated.[6,12] This technique can provide anywhere from a few monolayers of graphene to several (>50) layers on the surface of a SiC wafer. Graphene layers grown by this technique have demonstrated low temperature carrier mobilities in the few tens of thousand $cm^2/V\ s$ range.[6] In addition, the electronic and phononic properties of epitaxially grown graphene multilayers have been found to be different from those of bulk graphite and similar to those of a graphene monolayer.[13–16] The exact structure of epitaxial graphene and the nature of interlayer couplings remain active areas of investigation. Measurement of the optical absorption spectra over a wide frequency range can provide useful information about the structure of epitaxial graphene.

In the visible to the mid-IR wavelength range ($\lambda < 10\ \mu m$), the optical absorption spectra of exfoliated graphene monolayers have been reported recently.[17–19] In this paper, we report results from measurements of the optical absorption spectra of epitaxial graphene from the visible to the terahertz frequency range for the first time and compare the results with the theoretical predictions for graphene. In graphene, the valence and conduction bands resulting from the mixing of the p_z-orbitals are degenerate at the K (K') points of the Brillouin zone. Near these points, the tight-binding Hamiltonian can be linearized and written as[1]

$$H = \begin{bmatrix} \Delta & \hbar v(k_x + ik_y) \\ \hbar v(k_x - ik_y) & -\Delta \end{bmatrix}, \tag{1}$$

where $v \approx 10^6$ m/s is the Fermi velocity. This Hamiltonian results in the energy dispersion relation for the conduction and valence bands given by $E_V^c(k) = \pm\sqrt{\Delta^2 + (\hbar v k)^2}$. The bandgap is equal to 2Δ and could acquire a nonzero value as a result of any interaction that breaks the symmetry between the A and B atoms in the unit cell of graphene. Optical absorption in graphene is described by the optical conductivity $\sigma(\omega)$. It can be written as the sum of the interband conductivity $\sigma_{\text{inter}}(\omega)$ and the intraband conductivity $\sigma_{\text{intra}}(\omega)$, both of which can be found using the Hamiltonian above and are given below:[10,20,21]

$$\sigma_{\text{inter}}(\omega) = i\frac{e^2\omega}{\pi}\int_{\Delta}^{\infty} d\epsilon \frac{(1+\Delta^2/\epsilon^2)}{(2\epsilon)^2 - (\hbar\omega + i\Gamma)^2} \times [f(\epsilon - E_F) - f(-\epsilon - E_F)], \tag{2}$$

$$\sigma_{\text{intra}}(\omega) = i\frac{e^2/\pi\hbar^2}{\omega + i/\tau}\int_{\Delta}^{\infty} d\epsilon (1+\Delta^2/\epsilon^2) \times [f(\epsilon - E_F) + f(\epsilon + E_F)]. \tag{3}$$

Here, $f(\epsilon - E_F)$ is the Fermi distribution function with Fermi energy E_F, Γ describes the broadening of the interband transitions, and τ is the momentum relaxation time due to carrier intraband scattering. The frequency dependencies of the real parts of $\sigma_{\text{inter}}(\omega)$ and $\sigma_{\text{intra}}(\omega)$ are depicted in Fig. 1; assuming $\Delta = 0$, $\Gamma = 10$ meV, and $T = 300$ K. Figure 1(a) shows the conductivities for $E_F = -100$ meV and two different values of the scattering time $\tau = 25$ and 5 fs. Figure 1(b) shows the conductivities for $\tau = 25$ fs and two different values of the Fermi energy $E_F = 0$ and -100 meV. At large frequencies, the real part of $\sigma_{\text{inter}}(\omega)$ has a constant value equal to $e^2/4\hbar$. At small frequencies, the real part of $\sigma_{\text{inter}}(\omega)$ approaches zero because interband optical transitions are blocked due to the presence of electrons and holes near the band edges. The plasmon dispersion and the free-carrier absorption in graphene are described by $\sigma_{\text{intra}}(\omega)$. Its frequency dependence is similar to that of a Drude model, as it is evident

[a]Electronic mail: jd234@cornell.edu.

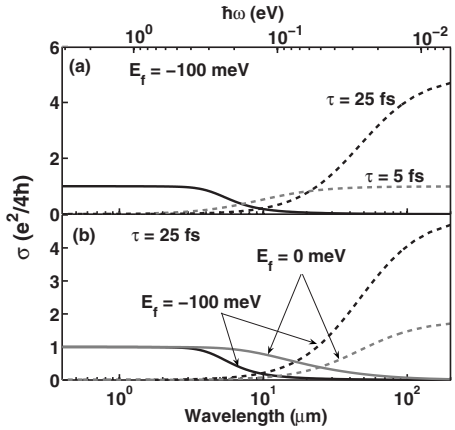

FIG. 1. Real parts of the interband (solid) and intraband (dashed) optical conductivities of graphene are plotted. (a) $E_F=-100$ meV and $\tau=25$ and 5 fs. (b) $\tau=25$ fs and $E_f=0$ and -100 meV. Values of Γ and Δ are assumed to be 10 and 0 meV, respectively, and $T=300$ K.

from the prefactor in Eq. (3). Figure 1(b) shows that the spectral shape of $\sigma_{\text{intra}}(\omega)$ at small frequencies is strongly influenced by the intraband carrier scattering time τ. The total conductivity $\sigma(\omega)$ has a minimum in the frequency range where both $\sigma_{\text{intra}}(\omega)$ and $\sigma_{\text{inter}}(\omega)$ are small.

The epitaxial graphene samples used in this work were grown on the carbon face of semi-insulating 6*H*-SiC wafers using the techniques that have been reported in detail previously.[12] The samples were grown at temperatures of 1400–1600 °C and pressures of $2-7\times10^{-6}$ torr. The number of carbon atom layers in each sample were estimated through x-ray photoelectron spectroscopy (XPS) using the Thickogram method.[22] Raman spectroscopy (using excitation wavelength of 488 nm) of the samples showed the characteristic *G* and *D* peaks near 1580 $\text{cm}^{-1}$and 1350 cm^{-1}, respectively. The ratio of the intensities of the *G* and *D* peaks (I_G/I_D) has been shown to be proportional to the crystal coherence length.[23,24] The ratio I_G/I_D for samples A, B, and C were ~13, ~17, and ~1.6, respectively, indicating that sample C has a much larger level of disorder compared to the other two samples. Ultrafast carrier dynamics in samples A and B have been studied in a previous work.[24] Sample C reported in this paper is not the same as the one reported in our earlier study.[25]

Three different instruments were used to measure the optical transmission through the graphene samples. In the visible to the near-IR wavelength range (0.4–0.9 μm) a grating spectrometer was used. In the near-IR to the mid-IR range (1.4–25 μm) a mid-IR Fourier transform IR (FTIR) spectrometer was used. Also, in the mid-IR to the far-IR (terahertz) wavelength range (15–200 μm) a far-IR FTIR spectrometer was used. The measured transmission spectrum for each sample was normalized to the transmission spectrum of a reference SiC wafer. The SiC substrate transmits very little in the 6–14 μm wavelength range due to multiphonon absorption.[26] As a result, the measured transmission spectra had poor signal-to-noise ratios in this wavelength range. The fringes in the transmission spectra arising from multiple reflections within the SiC substrate were numerically filtered out after normalizing with respect to the transmission spectrum of the reference SiC wafer.

Figure 2 shows the normalized transmission spectra through the epitaxial graphene samples A, B, and C. The

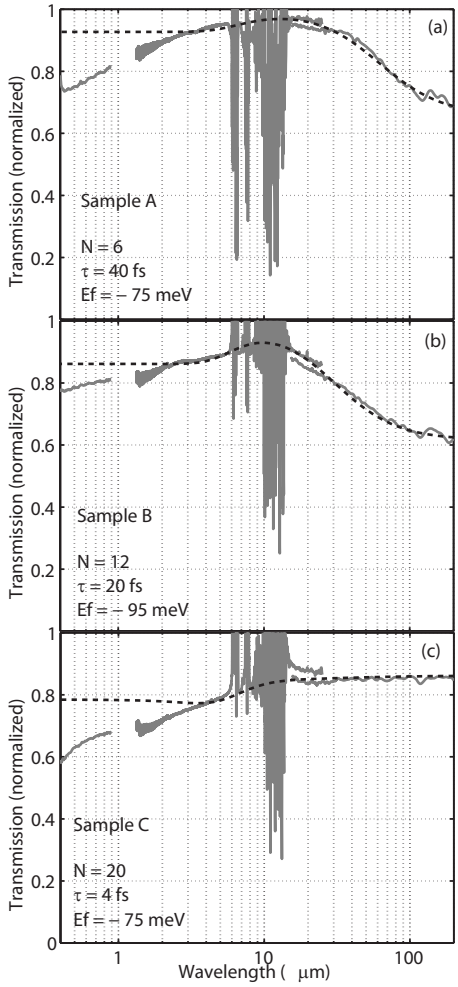

FIG. 2. Measured transmission spectra (solid gray lines) of samples A, B, and C from 0.4 to 200 μm along with the theoretical transmission spectra (dashed black line) using Eqs. (2)–(4). The values of the fitting parameters are included in the insets. The value of Δ is assumed to be zero.

optical absorption in the graphene layers depends sensitively on the substrate index of refraction. Matching the optical boundary conditions at the air/graphene/SiC interfaces, the optical transmission $T(\omega)$ through N graphene layers on a SiC wafer (normalized to the transmission through a plain SiC wafer) can be written in terms of the complex optical conductivity $\sigma(\omega)$ as

$$T(\omega)=\left|1+N\sigma(\omega)\sqrt{\mu_o/\epsilon_o}/(1+n_{\text{SiC}})\right|^{-2}, \tag{4}$$

where $n_{\text{SiC}}\sim2.55$ is the refractive index of SiC. For $N|\sigma(\omega)|\sqrt{\mu_o/\epsilon_o}/(1+n_{\text{SiC}})\ll1$, $T(\omega)$ is related to only the real part of the optical conductivity and can therefore be used to measure the absorption spectra of graphene. We have used Eqs. (2)–(4) to model the measured transmission data using N, τ, and E_F as the fitting parameters. The parameters Γ and Δ were assumed to be ~10 and ~0 meV, respectively. Changing the values of Γ and Δ by small amounts (much less than k_BT) had little effect on the final results. The dashed black lines in Fig. 2 are the theoretical fits to the experimental data (solid gray lines). The values of the fitting parameters are shown in the insets.

The number of graphene layers N obtained this way agrees well with the value obtained through XPS. For example, the XPS method gave values of $N=6$ and 11 for samples A and B, respectively. The extracted values of the

Fermi energy correspond to average carrier densities of $\sim 5 \times 10^{11}$ and $\sim 8 \times 10^{11}$ cm^{-2} per layer for samples A and B, respectively. Due to the electron-hole symmetry of the graphene bandstructure near the band edge, both negative and positive signs of the Fermi energy will fit the experimental data equally well. Also note that the experiments only give information on the total conductivity $N\sigma(\omega)$ of all the layers, and therefore, the extracted value of the Fermi energy should be taken as an average value for all the layers. Recent work on epitaxial graphene suggests that a concentration of carriers larger than the intrinsic value is expected only in the first few carbon atom layers near the SiC interface. Assuming that only the first two layers have nonzero Fermi levels and the remaining layers are intrinsic, values of the Fermi level equal to -150 and -290 meV for the first two layers of samples A and B, respectively, provide good fits to the measured data. The reason for the difference in the Fermi levels between the two samples is not well understood. It might be attributable to the differences in the growth conditions. As mentioned earlier, sample C is significantly more disordered than samples A and B. The transmission spectra of sample C show a distinctly different shape in the terahertz region (Fig. 2, sample C), which can be fitted well with a very short carrier scattering time of ~ 4 fs.

It has been recently pointed out that the first few graphene layers in epitaxially grown graphene could acquire a bandgap as a result of interaction with the atoms in the SiC substrate.[27] Although a value of Δ equal to zero was found to fit our measured data well, a value of Δ much smaller than $k_B T$ would be difficult to detect in our measurements. A nonzero value of the bandgap 2Δ in the mid-IR to far-IR range, where the intraband contribution to the conductivity dominates, would have little effect on the transmission spectra. If the value of the bandgap is in the near-IR to the mid-IR range, then its effects at room temperature would be hard to distinguish from the reduction in the interband conductivity at small frequencies due to band filling effects [see Fig. 1(b)]. Also, in multilayer graphene structures the optical response is dominated by the large number of layers that are not close to the substrate and do not have a bandgap.

The short wavelength end of the measured transmission spectra in Fig. 2 deviates from the theoretical predictions for wavelengths shorter than ~ 2.5 μm. The deviation is minimum for sample B and corresponds to $\sim 50\%$ more absorption at 0.4 μm compared to the theory. The reasons for this deviation are not clear. Two factors could be responsible for this behavior: (i) the band energy dispersion and interband optical matrix elements at large energies are different from those obtained from the Hamiltonian given in Eq. (2) and (ii) increased light scattering may be expected from the sample at shorter wavelengths as the wavelength approaches the crystal coherence length ($\sim 50-100$ nm). The band energy dispersion in epitaxial graphene at large energies could be affected by the nature of the interlayer couplings. Note that the deviation of the measured transmission spectra from the theory is not the same for the three samples indicating that disorder might also have a role to play. More work is needed to investigate the nature of this discrepancy.

In conclusion, we have measured the optical absorption spectra of epitaxial graphene from the terahertz to the visible frequencies. The experimental results have been shown to be in agreement with the theory except at short wavelengths. Our results confirm the Drude-like frequency dependence of the intraband conductivity of graphene in the terahertz frequency range. The results presented here indicate that absorption spectroscopy can be used as a noninvasive technique to characterize graphene films and find the values of parameters such as the Fermi energy and the carrier density, carrier intraband scattering time, and the number of graphene layers.

The authors acknowledge support from the National Science Foundation, the Air Force Office of Scientific Research (Contract No. FA9550–07–1–0332) (contract monitor Dr. Donald Silversmith), and Cornell Material Science and Engineering Center (CCMR) program of the National Science Foundation (Cooperative Agreement No. 0520404).

[1] R. Saito, G. Dresselhaus, and M. S. Dresselhaus, *Physical Properties of Carbon Nanotubes* (Imperial College, London, UK, 1999).
[2] A. H. Castro Neto, F. Guinea, N. M. R. Peres, K. S. Novoselov, and A. K. Geim, "The electronic properties of graphene," Rev. Mod. Phys. (submitted); Also available at e-print arXiv:cond-mat/0709.1163.
[3] K. S. Novoselov, A. K. Geim, S. V. Morozov, D. Jiang, M. I. Katsnelson, I. V. Grigorieva, S. V. Dubonos, and A. A. Firsov, Nature (London) **438**, 197 (2005).
[4] K. S. Novoselov, A. K. Geim, S. V. Morozov, D. Jiang, Y. Zhang, S. V. Dubonos, I. V. Grigorieva, and A. A. Firsov, Science **306**, 666 (2004).
[5] Y. Zhang, Y. Tan, H. L. Stormer, and P. Kim, Nature (London) **438**, 201 (2005).
[6] C. Berger, Z. Song, X. Li, X. Wu, N. Brown, C. Naud, D. Mayou, T. Li, J. Hass, A. N. Marchenkov, E. H. Conrad, P. N. First, and W. A. de Heer, Science **312**, 1191 (2006).
[7] G. Liang, N. Neophytou, D. E. Nikonov, and M. S. Lundstrom, IEEE Trans. Electron Devices **54**, 677 (2007).
[8] J. R. Williams, L. DiCarlo, and C. M. Marcus, Science **317**, 638 (2007).
[9] G. Gu, S. Nie, R. M. Feenstra, R. P. Devaty, W. J. Choyke, W. K. Chan, and M. G. Kane, Appl. Phys. Lett. **90**, 253507 (2007).
[10] F. Rana, IEEE Trans. Nanotechnol. **7**, 91 (2008).
[11] F. Schedin, A. K. Geim, S. V. Morozov, E. W. Hill, P. Blake, M. I. Katsnelson, and K. S. Novoselov, Nat. Mater. **6**, 652 (2007).
[12] C. Berger, Z. Song, T. Li, X. Li, A. Y. Ogbazghi, R. Feng, Z. Dai, A. N. Marchenkov, E. H. Conrad, P. N. First, and W. A. de Heer, J. Phys. Chem. B **108**, 19912 (2004).
[13] C. Faugeras, A. Nerriere, M. Potemski, A. Mahmood, E. Dujardin, C. Berger, and W. A. de Heer, Appl. Phys. Lett. **92**, 011914 (2008).
[14] J. Hass, F. Varchon, J. E. Millan-Otoya, M. Sprinkle, N. Sharma, W. A. de Heer, C. Berger, P. N. First, L. Magaud, and E. H. Conrad, Phys. Rev. Lett. **100**, 125504 (2008).
[15] S. Latil, V. Meunier, and L. Henrard, Phys. Rev. B **76**, 201402(R) (2007).
[16] J. M. B. Lopes dos Santos, N. M. R. Peres, and A. H. Castro Neto, Phys. Rev. Lett. **99**, 256802 (2007).
[17] Z. Q. Li, E. A. Henriksen, Z. Jiang, Z. Hao, M. C. Martin, P. Kim, H. L. Stormer, and D. N. Basov, Nat. Phys. **4**, 532 (2008).
[18] R. R. Nair, P. Blake, A. N. Grigorenko, K. S. Novoselov, T. J. Booth, T. Stauber, N. M. R. Peres, and A. K. Geim, Science **320**, 1308 (2008).
[19] K. F. Mak, M. Sfeir, Y. Wu, C. H. Lui, J. Maultzsch, S. Rosenblatt, M. Hybertsen, and T. Heinz, Bull. Am. Phys. Soc. **53**, L29.3 (2008).
[20] V. P. Gusynin, S. G. Sharapov, and J. P. Carbotte, Phys. Rev. Lett. **96**, 256802 (2006); V. P. Gusynin, J. Phys.: Condens. Matter **19**, 026222 (2007).
[21] N. M. R. Peres, F. Guinea, and A. H. Castro Neto, Phys. Rev. B **73**, 125411 (2006).
[22] P. J. Cumpson, Surf. Interface Anal. **29**, 403 (2000).
[23] A. C. Ferrari, J. C. Meyer, V. Scardaci, C. Casiraghi, M. Lazzeri, F. Mauri, S. Piscanec, D. Jiang, K. S. Novoselov, S. Roth, and A. K. Geim, Phys. Rev. Lett. **97**, 187401 (2006).
[24] A. C. Ferrari and J. Robertson, Phys. Rev. B **61**, 14095 (2000).
[25] J. M. Dawlaty, S. Shivaraman, M. Chandrashekhar, F. Rana, and M. G. Spencer, Appl. Phys. Lett. **92**, 042116 (2008).
[26] A. S. Bakin, S. I. Dorozhkin, and A. S. Zubrilov, Proceedings of the Fourth International High Temperature Electronics Conference (HITEC), 1998 (unpublished), pp. 253–256.
[27] S. Y. Zhou, G. H. Gweon, A. V. Fedorov, P. N. First, W. A. de Heer, D. H. Lee, F. Guinea, A. H. Castro Neto, and A. Lanzara, Nat. Mater. **6**, 770 (2007).